# Understanding Structural and Dynamic Properties of Well-Defined Rhenium-Based Olefin Metathesis Catalysts, Re(≡CR)(=CHR)(X)(Y), from DFT and QM/MM Calculations

Xavier Solans-Monfort,[†] Eric Clot,[†] Christophe Copéret,*[,‡] and Odile Eisenstein*[,†]

*LSDSMS (UMR 5636 CNRS-UM2), cc14, Institut Gerhardt, Université Montpellier 2, F-34095 Montpellier Cedex 05, France, and LCOMS (UMR 9986 CNRS-CPELyon), 43, CPE Lyon, Bd du 11 Novembre 1918, F-69616 Villeurbanne Cedex, France*

*Received December 17, 2004*

DFT(B3PW91) and QM/MM (B3PW91:UFF) calculations have been carried out to rationalize the structural and dynamical properties of quasi-tetrahedral alkylidyne-alkylidene rhenium complexes Re(CR)(CHR)(X)(Y) (R = alkyl, X = Y = alkyl; X = alkyl, Y = siloxy; X = Y = alkoxy), which are catalysts for olefin metathesis with efficiency depending on X and Y. The optimized geometries of all complexes are pseudo-tetrahedral and yield *syn* and *anti* isomers. The presence of the C−H agostic interaction in the *syn* isomers is evidenced by geometrical features as well as the $\nu_{C-H}$ stretching frequencies and $J_{C-H}$ NMR coupling constants calculated to be lower than in the *anti* isomers, as observed experimentally in the case of the $J_{C-H}$. Ancillary X and Y ligands that are weak $\sigma$-donors and $\pi$-donors (OR) compete with the agostic interaction. The calculated *syn*/*anti* ratios are in good agreement with experimental data. The *syn*/*anti* interconversion occurs preferentially via the alkylidene rotation, while H transfers between perhydrocarbyl ligands have much higher energy barriers, showing that this process does not compete with alkylidene rotation. Molecular orbital, natural bonding orbital (NBO), and Bader atoms-in-molecules (AIM) analyses have been carried out to rationalize the results.

## Introduction

Electron-deficient species are potential catalysts for a number of chemical transformations because of their electrophilic behavior toward an incoming organic ligand. For this reason early transition metal $d^0$ complexes are especially interesting targets. Of these systems, well-defined $d^0$ nucleophilic alkylidene metal complexes, also known as Schrock alkylidene complexes, can be highly efficient catalysts for olefin metathesis, when proper sets of ligands and metal are used.[1−5] While molybdenum- and tungsten-based catalysts have been shown to be efficient and are most commonly used,[6−12] well-defined Re-based catalysts, Re(≡CR)(=CHR)(X)(Y), are also active and usually more compatible with functional groups such as esters (Scheme 1, R = *t*Bu, X,Y = $CH_2$*t*Bu or OR).[13−19] The catalytic efficiency is highly influenced by the nature of the ancillary ligands and the surrounding media. For example, the Re complexes are active only when X and Y are O*t*Bu$_{6F}$ [OCMe(CF$_3$)$_2$],[15,16,20] albeit with a lower rate than their Mo and W analogues. More recently, a well-defined silica-supported Re complex, [(≡OSi)Re(≡C*t*Bu)(=CH*t*Bu)(CH$_2$*t*Bu)], has been reported, and it has shown unprecedented activity in olefin metathesis even compared with the Mo- and W-based homogeneous catalysts.[21−24]

All the Re-based catalyst precursors, Re(≡CR)(=CHR)(X)(Y), have several common structural characteristics: they have a pseudo-tetrahedral geometry,

* To whom correspondence should be addressed. E-mail: coperet@cpe.fr; odile.eisenstein@univ-montp2.fr.
† LSDSMS (UMR 5636 CNRS-UM2).
‡ LCOMS (UMR 9986 CNRS-CPELyon).

(1) Grubbs, R. H.; Chang, S. *Tetrahedron* **1998**, *54*, 4413.
(2) Fürstner, A. *Angew. Chem., Int. Ed.* **2000**, *39*, 3012.
(3) Buchmeiser, M. R. *Chem. Rev.* **2000**, *100*, 1565.
(4) Schrock, R. R.; Hoveyda, A. H. *Angew. Chem., Int. Ed.* **2003**, *42*, 4592.
(5) Schrock, R. R. *Top. Organomet. Chem.* **1998**, *1*, 1.
(6) Schrock, R. R. *Acc. Chem. Res.* **1986**, *19*, 342.
(7) Schrock, R. R. *Acc. Chem. Res.* **1990**, *23*, 158.
(8) Schrock, R. R. *Polyhedron* **1995**, *14*, 3177.
(9) Kress, J.; Wesolek, M.; Osborn, J. *J. Chem. Soc., Chem. Commun.* **1982**, 514.
(10) Kress, J.; Osborn, J. *J. Am. Chem. Soc.* **1983**, *105*, 6346.
(11) Kress, J.; Osborn, J. *Angew. Chem., Int. Ed. Engl.* **1992**, *31*, 1585.
(12) Lefebvre, F.; Leconte, M.; Pagano, S.; Mutch, A.; Basset, J.-M. *Polyhedron* **1995**, *14*, 3209.
(13) Edwards, D. S.; Schrock, R. R. *J. Am. Chem. Soc.* **1982**, *104*, 6806.
(14) Edwards, D. S.; Vollaro Biondi, L.; Ziller, J. W.; Churchill, M. R.; Schrock, R. R. *Organometallics* **1983**, *2*, 1505.
(15) Toreki, R.; Schrock, R. R. *J. Am. Chem. Soc.* **1990**, *112*, 2448.
(16) Toreki, R.; Schrock, R. R., Vale, M. G. *J. Am. Chem. Soc.* **1991**, *113*, 3610.
(17) Toreki, R.; Schrock, R. R.; Davis, W. M. *J. Am. Chem. Soc.* **1992**, *114*, 3367.
(18) Toreki, R.; Vaughan, G. A.; Schrock, R. R.; Davis, W. M. *J. Am. Chem. Soc.* **1993**, *115*, 127.
(19) LaPointe, A. M.; Schrock, R. R. *Organometallics* **1995**, *14*, 1875.
(20) Schrock, R. R. *Chem. Rev.* **2002**, *102*, 145.
(21) Chabanas, M.; Copéret, C.; Basset, J.-M. *Chem. Eur. J.* **2003**, *9*, 971.
(22) Copéret, C. *New J. Chem.* **2004**, *28*, 1.
(23) Chabanas, M.; Baudouin, A.; Copéret, C.; Basset, J.-M. *J. Am. Chem. Soc.* **2001**, *123*, 2062.
(24) Copéret, C.; Chabanas, M.; Petroff Saint-Arroman, R.; Basset, J.-M. *Angew. Chem., Int. Ed.* **2003**, *42*, 156.

10.1021/om048997s CCC: $30.25 
Publication on Web 03/01/2005

**Scheme 1. *syn* (left) and *anti* (right) Isomers for Re(≡CR)(=CHR)(X)(Y)**

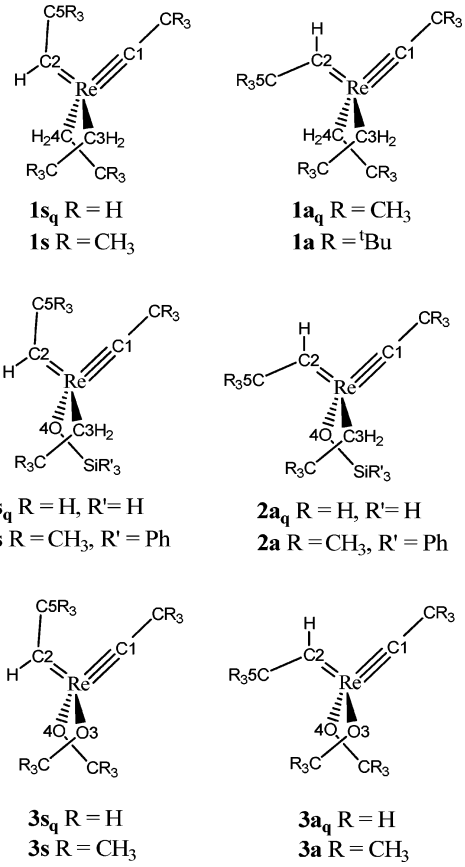


and they contain both alkylidyne and alkylidene ligands with their respective substituents being coplanar. As a consequence, two isomers have been observed in which the alkyl substituent of the alkylidene ligand points either toward or away from the alkylidyne, thus leading to *syn* and *anti* isomers, respectively (Scheme 1).

It has been observed that the *syn* isomers present a much lower $J_{C-H}$ coupling constant for their alkylidene proton (115−120 Hz) (as compared to that of their respective *anti* isomers: 160−180 Hz),[17,25,26] and this has been associated with an elongation of the C−H bond and therefore with the presence of an α-agostic interaction.[27−29] However, it is currently recognized that an α-agostic C−H interaction is not favored in a tetrahedral complex.[30] Yet, similar low *syn* $J_{C-H}$ values have been reported for the isolobal [Mo(=NR)(=CHR′)(OR″)$_2$] complexes, which lead the authors to suggest the existence of an α-C−H agostic interaction.[31−34]

**Scheme 2. Schematic Representation of the Rotation of the Alkylidene Ligand and of the Reaction Paths for H Transfer between Ligands**

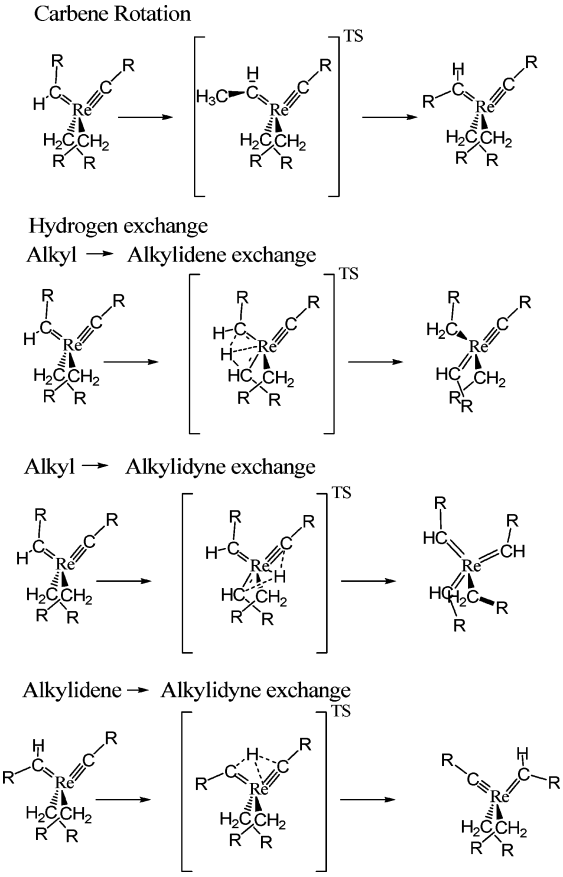


The *syn* and *anti* isomers (rotamers) interconvert slowly, and their thermodynamic ratio, as well as their rate of interconversion, depend on the nature of the substituents X and Y. For example, when X and Y are $CH_2t$Bu, the *syn* isomer is the only one observed,[35] whereas when X and Y are O*t*Bu, the two isomers are present, the *anti* isomer being the major one (75%).[17] For Re(≡C*t*Bu)(=CH*t*Bu)(OR)$_2$, the isomerization requires several hours at 100 °C or higher temperatures and is attributed to the alkylidene rotation.[20] The enthalpy barrier increases when the alkoxy group is substituted by fluorine atoms (19.5, 23.4, and 25.5 kcal mol$^{-1}$ for R = *t*Bu, [CMe$_2$(CF$_3$)], and [CMe(CF$_3$)$_2$], respectively).[17] The high rotation barrier of the alkylidene ligand has been suggested to be associated with the loss of a metal−alkylidyne π bond in the transition state: when the alkylidene ligand is rotated by 90°, the alkylidyne and alkylidene π orbitals compete for the same metal d orbital.[17] Another characteristic of these complexes is the extremely slow H transfer (weeks) between the alkylidene and alkylidyne ligands and between the neopentyl and any of the unsaturated ligands,[19,26,36] which could also be related to *syn*−*anti* isomerization (Scheme 2).

(25) Lesage, A.; Emsley, L.; Chabanas, M.; Copéret, C.; Basset, J.-M. *Angew. Chem., Int. Ed.* **2002**, *41*, 4535.
(26) Chabanas, M.; Baudouin, A.; Copéret, C.; Basset, J.-M.; Lukens, W.; Lesage, A.; Hediger, S.; Emsley, L. *J. Am. Chem. Soc.* **2003**, *125*, 492.
(27) Brookhart, M.; Green, M. L. H. *J. Organomet. Chem.* **1983** *250*, 395.
(28) Brookhart, M.; Green, M. L. H.; Wong, L.-L. *Prog. Inorg. Chem.* **1988**, *36*, 1.
(29) Kubas G. J. *Metal Dihydrogen and σ-Bond Complexes: Structure, Theory and Reactivity*; Kluwer Academic Publishers: New York, 2001, and references therein.
(30) Eisenstein, O.; Jean, Y. *J. Am. Chem. Soc.* **1985**, *107*, 1177.
(31) Oskam, J. H.; Schrock, R. R. *J. Am. Chem. Soc.* **1993**, *115*, 11831.
(32) Schrock, R. R.; Murdzek, J. S.; Bazan, G. C.; Robbins, J.; DiMare, M.; O'Regan, M. *J. Am. Chem. Soc.* **1990**, *112*, 3875.
(33) Fox, H. H.; Schofield, M. H.; Schrock, R. R. *Organometallics* **1994**, *13*, 2804.
(34) Schrock, R. R.; Crowe, W. E.; Bazan, G. C.; DiMare, M.; O'Regan, M. B.; Schofield, M. H. *Organometallics* **1991**, *10*, 1832.
(35) Chabanas, M. PhD Thesis, Université Claude Bernard Lyon I, 2001.
(36) Caulton, K. G.; Chisholm, M. H.; Streib, W. E.; Xue, Z. *J. Am. Chem. Soc.* **1991**, *113*, 6082.

Because these systems are good olefin metathesis catalysts, we have decided to investigate in detail the origin of these special structural features, which are not fully understood. Computational studies at the Hartree−Fock and SCF-Xα-SW levels on the related Mo and W imidoalkylidene systems have been reported and focused on the rotational barrier of the alkylidene ligand.[33,37]

In this paper, we have carried out DFT and QM/MM studies of the structural and dynamic properties of several Re(≡CR)(=CHR)(X)(Y) complexes. Computational studies of the agostic interaction have been carried out on numerous systems, and the various factors involved have been discussed. The computational effort on this interaction has recently been reviewed.[38] Despite the relative weakness of the C−H agostic interactions, DFT methods have been shown to be appropriate for geometry optimization. The agostic interaction is sensitive to steric factors, and the need to take into account the full identity of the complexes has been recognized.[38] The QM/MM methods are thus methods of choice for the study of large systems.

## Computational Details

Two sets of calculations were carried out to represent the experimental rhenium Re(≡C*t*Bu)(=CH*t*Bu)(X)(Y) complexes (X = Y = $CH_2$*t*Bu, **1**; X = $CH_2$*t*Bu, Y = $OSiPh_3$, **2**; X = Y = O*t*Bu, **3**; see Scheme 1). For **1**−**3**, the *t*Bu group was substituted by a methyl and the phenyl group by a hydrogen atom in the QM calculations. The hybrid B3PW91[39,40] density functional, as implemented in the Gaussian98[41] and Gaussian03[42] packages, was used in the QM calculations. The Re and Si atoms were represented with the quasirelativistic effective core pseudopotentials (RECP) of the Stuttgart group and the associated basis sets augmented with a polarization function (α = 0.869, Re; α = 0.284, Si).[43,44] The remaining atoms (C, H, and O) were represented with 6-31G(d,p) basis sets.[45] To test the basis set accuracy, single-point calculations were carried out with the same representation for Re and Si and a 6-311++G(2df,2pd) basis set for C, H, and O.[46] Moreover, geometry optimizations for Re(≡$CCH_3$)(=$CHCH_3$)($CH_2CH_3$)$_2$ were performed with the large basis set. Both tests showed no significant changes in the results with the larger basis sets. Therefore only the results with the smaller basis set are reported.

To test the steric influence of the *t*Bu groups, ONIOM[47] (B3PW91:UFF) calculations were performed on the experimental systems. The inner layer (QM) is the same as described above, and the outer layer (MM) treats the missing groups (Me and Ph) with molecular mechanics calculations using the UFF force field.[48] To differentiate between QM and QM/MM calculations, all complexes computed at the QM level are designed with an added **q** subscript. A further distinction is made according to the position of the alkylidene C−R bond with respect to the alkylidyne ligand (**s** for *syn* and **a** for *anti*, see Scheme 1). Test calculations were carried out for complex **1** to assess the reliability of the ONIOM approximation. Single-point calculations on the ONIOM geometries gave a difference in energy between the *syn* and *anti* isomers that differs from that at the QM/MM level by only 0.2 kcal mol$^{-1}$. Furthermore, a geometry optimization at the DFT level gave geometrical and energy results similar to that with ONIOM.

The B3PW91 and ONIOM (B3PW91:UFF) geometry optimizations were performed without any symmetry constraints, and the nature of the extrema (local minima or transition states) was checked by analytical frequency calculations. The harmonic $\nu_{C-H}$ stretching frequency of the alkylidene C−H bond has been identified as an isolated mode in the calculations. The energies discussed throughout the text are electronic energies without any ZPE corrections. Gibbs free energies have been computed from harmonic frequencies at 298.15 K and 1 atm. In addition, the NMR $J_{C-H}$ coupling constants of the alkylidene C−H bond have only been computed for the QM model at the B3PW91 level using the methodology implemented in the Gaussian03 package.[49]

The wave function of the complexes was analyzed through a natural bonding orbital (NBO) scheme[50] that enables the description of bonds between atoms as a linear combination of hybrids located on each partner of the bond. The natural population analysis (NPA)[50] was used to estimate the atomic charges. The topological properties of the electron density were also analyzed using Bader's atoms-in-molecules theory (AIM).[51,52]

## Results and Discussion

**Geometrical Structure of Re(≡CtBu)(=CHtBu)(X)(Y).** We have optimized the structures of Re(≡C*t*Bu)(=CH*t*Bu)($CH_2$*t*Bu)$_2$ (**1**), Re(≡C*t*Bu)(=CH*t*Bu)($CH_2$*t*Bu)($OSiPh_3$) (**2**), and Re(≡C*t*Bu)(=CH*t*Bu)(O*t*Bu)$_2$ (**3**) complexes. The complex **2** has been chosen because it has

(37) Cundari T. R.; Gordon, M. S. *Organometallics* **1992**, *11*, 55.
(38) Clot, E.; Eisenstein, O. In *Structure and Bonding, Computational Inorganic Chemistry*; Kaltzoyannis, N. McGrady, J. E., Eds.; Springer-Verlag: Heidelberg, 2004; pp 1−36, and references therein.
(39) Becke, A. D. *J. Chem. Phys.* **1993**, *98*, 5648.
(40) Perdew, J. P.; Wang, Y. *Phys. Rev. B* **1992**, *45*, 13244.
(41) Frisch, M. J.; Trucks, G. W.; Schlegel, H. B.; Scuseria, G. E.; Robb, M. A.; Cheeseman, J. R.; Zakrzewski, V. G.; Montgomery, J. A.; Stratmann, R. E.; Burant, J. C.; Dapprich, S.; Millam, J. M.; Daniels, A. D.; Kudin, K. N.; Strain, M. C.; Farkas, O.; Tomasi, J.; Barone, V.; Cossi, M.; Cammi, R.; Mennucci, B.; Pomelli, C.; Adamo, C.; Clifford, S.; Ochterski, J.; Petersson, G. A.; Ayala, P. Y.; Cui, Q.; Morokuma, K.; Malick, D. K.; Rabuck, A. D.; Raghavachari, K.; Foresman, J. B.; Cioslowski, J.; Ortiz, J. V.; Baboul, A. G.; Stefanov, B. B.; Liu, G.; Liashenko, A.; Piskorz P., Komaromi, I.; Gomperts, G.; Martin, R. L.; Fox, D. J.; Keith, T.; Al-Laham, M. A.; Peng, C. Y.; Nanayakkara, A.; Gonzalez, C.; Challacombe, M.; Gill, P. M. W.; Johnson, B. G.; Chen, W.; Wong, M. W.; Andres J. L.; Head-Gordon, M.; Replogle, E. S.; Pople J. A. *Gaussian 98*; Gaussian Inc.: Pittsburgh, PA, 1998.
(42) Frisch, M. J.; Trucks, G. W.; Schlegel, H. B.; Scuseria, G. E.; Robb, M. A.; Cheeseman, J. R.; Montgomery, J. A., Jr.; Vreven, T.; Kudin, K. N.; Burant, J. C.; Millam, J. M.; Iyengar, S. S.; Tomasi, J.; Barone, V.; Mennucci, B.; Cossi, M.; Scalmani, G.; Rega, N.; Petersson, G. A.; Nakatsuji, H.; Hada, M.; Ehara, M.; Toyota, K.; Fukuda, R.; Hasegawa, J.; Ishida, M.; Nakajima, T.; Honda, Y.; Kitao, O.; Nakai, H.; Klene, M.; Li, X.; Knox, J. E.; Hratchian, H. P.; Cross, J. B.; Adamo, C.; Jaramillo, J.; Gomperts, R.; Stratmann, R. E.; Yazyev, O.; Austin, A. J.; Cammi, R.; Pomelli, C.; Ochterski, J. W.; Ayala, P. Y.; Morokuma, K.; Voth, G. A.; Salvador, P.; Dannenberg, J. J.; Zakrzewski, V. G.; Dapprich, S.; Daniels, A. D.; Strain, M. C.; Farkas, O.; Malick, D. K.; Rabuck, A. D.; Raghavachari, K.; Foresman, J. B.; Ortiz, J. V.; Cui, Q.; Baboul, A. G.; Clifford, S.; Cioslowski, J.; Stefanov, B. B.; Liu, G.; Liashenko, A.; Piskorz, P.; Komaromi, I.; Martin, R. L.; Fox, D. J.; Keith, T.; Al-Laham, M. A.; Peng, C. Y.; Nanayakkara, A.; Challacombe, M.; Gill, P. M. W.; Johnson, B.; Chen, W.; Wong, M. W.; Gonzalez, C.; Pople, J. A.; *Gaussian 03*; Gaussian, Inc.: Wallingford, CT, 2004.
(43) Andrae, D.; Häussermann, U.; Dolg, M.; Stoll, H.; Preuss, H. *Theor. Chim. Acta* **1990**, *77*, 123.
(44) Bergner, A.; Dolg, M.; Küchle, W.; Stoll, H.; Preuss, H. *Mol. Phys.* **1990**, *30*, 1431.
(45) Hehre, W. J.; Ditchfield, R.; Pople, J. A. *J. Chem. Phys.* **1972**, *56*, 2257.
(46) Krishnan, R.; Binkley, J. S.; Seeger, R.; Pople, J. A. *J. Chem. Phys.* **1980**, *72*, 650.
(47) Svensson, M.; Humbel, S.; Froese, R. D. J.; Matsubara, T.; Sieber, S.; Morokuma, K. *J. Phys. Chem.* **1996**, *100*, 19357.
(48) Rappé, A. K.; Casewitt, C. J.; Colwell, K. S.; Goddard, W. A., III; Skiff, W. M. *J. Am. Chem. Soc.* **1992**, *114*, 10024.
(49) Helgaker, T.; Watson, M.; Handy, N. C. *J. Chem. Phys.* **2000**, *113*, 9402.
(50) Reed, A. E.; Curtiss, L. A.; Weinhold, F. *Chem. Rev.* **1988**, *88*, 899.
(51) Bader, R. F. *Atoms in Molecules. A Quantum Theory*; Oxford University Press: Oxford, UK, 1990.
(52) Bader, R. F. *Chem. Rev.* **1991**, *91*, 893.

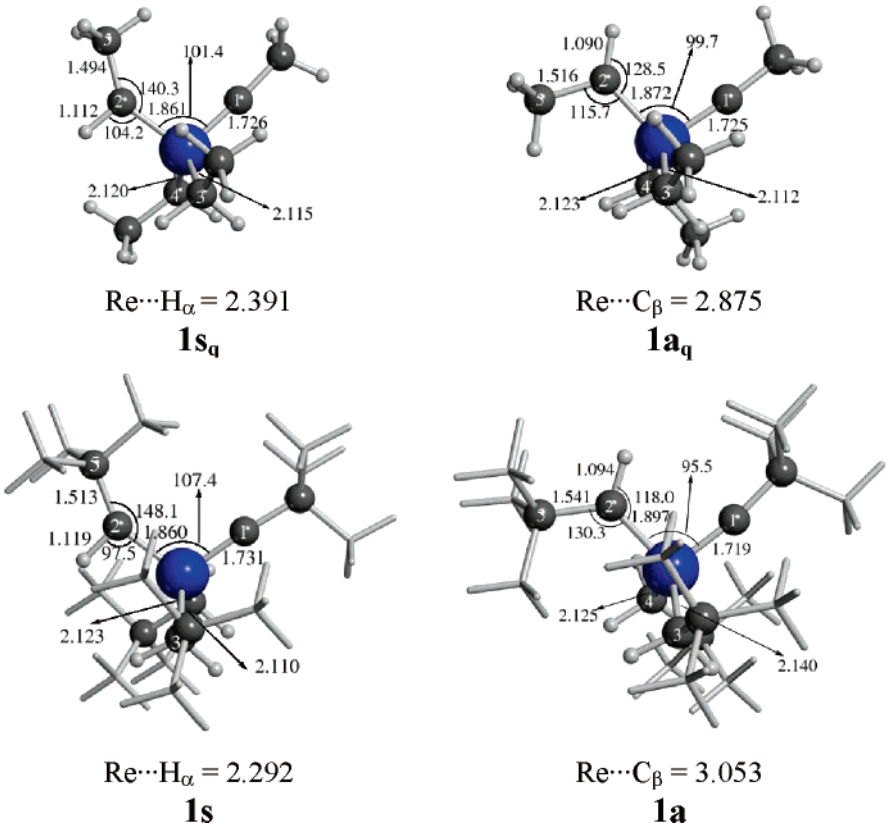


**Figure 1.** Optimized structures of Re(≡CR)(=CHR)$(CH_2R)_2$ using QM (**1s$_q$**, **1a$_q$**) and QM/MM (**1s**, **1a**) models. Distances in Å and angles in deg.

**Table 1. Energies and Gibbs Free Energies, in kcal mol$^{-1}$, Relative to the More Stable Isomer, Unscaled Stretching Frequencies for C2−H ($\nu_{C-H}$) and C2−C5 ($\nu_{C-C}$) in cm$^{-1}$, and Calculated C2−H NMR Coupling Constants ($J_{C-H}$) in Hz for Re(≡C*t*Bu)(=CH*t*Bu)$(CH_2tBu)_2$ *syn* and *anti* Isomers (experimental $J_{C-H}$ value is added)**

| structure[a] | $\Delta E / \Delta G^\circ_{298}$ | *syn*/*anti*% calc[b] | *syn*/*anti* % exptl | $\nu_{C-H}$ calc | $\nu_{C-C}$ calc | $J_{C-H}$ calc | $J_{C-H}$ exptl |
|---|---|---|---|---|---|---|---|
| **1s$_q$** | 0.0 / 0.0 | 98 / 98 | | 2932 | 1147 | 138 | |
| **1a$_q$** | 2.2 / 2.4 | 2 / 2 | not obsd | 3160 | 1051 | 175 | |
| **1s** | 0.0 / 0.0 | 99 / 100 | | 2877 | 1087 | | 115[58] |
| **1a** | 2.7 / 3.5 | 1 / 0 | not obsd | 3117 | 1037 | | |

[a] See Figure 1. [b] Calculated from $\Delta E/\Delta G^\circ_{298}$.

the same spectroscopic characteristics as the surface complex (≡SiO)Re(≡C*t*Bu)(=CH*t*Bu)$(CH_2tBu)$.[26]

Figure 1 shows the optimized geometries of the *syn* and *anti* isomers of Re(=CR)(=CHR)$(CH_2R)_2$ with both QM (**1s$_q$** and **1a$_q$**, R = $CH_3$) and QM/MM (**1s** and **1a**, R = *t*Bu) models. Table 1 gives their relative energies and selected spectroscopic properties. Species **1s$_q$** and **1a$_q$** present a pseudo-tetrahedral coordination at Re, the angle between the alkylidene and alkylidyne ligands being smaller (ca. 100°) than 109°. Substituents of the alkylidene and the alkylidyne are coplanar; rotating the alkylidene by 90° around the Re=C bond does not yield a local minimum and the geometries presented in Figure 1 are recovered. The Re−C distances for the alkylidyne and alkylidene ligands are very close to those obtained in the solid state structure for a closely related complex, *anti* Re(≡C*t*Bu)(=CHFc)$(OCMe(CF_3)_2)_2$ (Fc = ferrocenyl).[18] Isomer **1s$_q$** presents a small Re−C2−H angle (104.2°) and a long C2−H bond (1.112 Å), associated with a rather short Re···H distance of 2.391 Å, which are indicative of a weak α-C−H agostic interaction. Remarkably, the *anti* isomer (**1a$_q$**) exhibits an angle Re−C2−C5 of less than 120° (115.7°), a longer C2−C5 distance than in **1s$_q$** (1.516 vs 1.494 Å) associated with a rather short Re···C5 distance (2.875 Å as compared with that in **1s$_q$**, i.e., 3.158 Å), suggestive of a weak α-C−C agostic interaction. The lack of bulky ligands in these model complexes suggests that the α-agostic interactions are driven by electronic factors. These features indicate that these $Re^{VII}$ complexes have a different electronic structure from the eight-electron tetrahedral complex $Cl_3TiCH_3$, which does not show any α-C−H agostic interaction.[30] The C−C agostic interaction is rare in systems without any geometrical constraint,[53,54] but a small angle Re=$C_\alpha$−$C_\beta$, i.e., 114°, in *anti* Re(≡C*t*Bu)(=CHFc)$(OCMe(CF_3)_2)_2$ (Fc = ferrocenyl) has been observed and can be interpreted as a signature of a C−C agostic interaction.[18]

Inclusion of the bulky ligands in QM/MM calculations of the full complexes does not alter the main results

(53) Jaffart, J.; Etienne, M.; Reinhold, M.; McGrady, J. E.; Maseras, F. *Chem. Commun.* **2003**, 876.
(54) Jaffart, J.; Cole, M. L.; Etienne, M.; Reinhold, M.; McGrady, J. E.; Maseras, F. *Dalton Trans.* **2003**, 4057.

obtained with the smaller models (Figure 1). The pseudo-tetrahedral geometry is maintained, and the agostic interaction is still present. The most important change observed for **1s** is the opening of the C2−Re−C1 angle (107.4°) compared with the value of 101.4° in $\mathbf{1s_q}$. This angle opening comes from steric repulsions between the *t*Bu groups of the alkylidene and alkylidyne ligands. This, in turn, reinforces the α-agostic interaction on the alkylidene: the Re−C2−H angle decreases to 97.5°, the C2−H bond length increases to 1.119 Å, and the Re···H distance becomes shorter (2.292 Å). For **1a**, an opposite distortion is observed: the Re−C2−C5 becomes larger (130.3° vs 115.7°), and the C2−Re−C1 angle becomes smaller (95.5° vs 99.7°). These two angular changes decrease the steric repulsion between the *t*Bu ligands, which results in the loss of the C−C agostic interaction.

The vibrational C−H stretching frequency, $\nu_{C-H}$, and the NMR coupling constants, $J_{C-H}$, have been calculated (Table 1). The computed $\nu_{C-H}$ values are slightly larger in $\mathbf{1_q}$ than in **1**. The stretching $\nu_{C-H}$ is isolated from the other modes, and after scaling by 0.9573,[55] to account for both systematic errors on the calculation of the force constant and the lack of anharmonic effects, the resulting values (2807 and 2754 $cm^{-1}$ for $\mathbf{1s_q}$ and **1s**, respectively) fall near the upper limit of the range of values characteristic of agostic C−H interactions. However, the lack of experimental values for the alkylidene C−H bond does not allow further comparison with these calculated values. The presence of an α-C−H agostic interaction in the *syn* isomer is evidenced by the lower $\nu_{C-H}$ stretching frequencies (about 230 $cm^{-1}$) for either $\mathbf{1s_q}$ or **1s** than those corresponding to *anti* isomers, $\mathbf{1a_q}$ and **1a**, respectively. The computed $J_{C-H}$ values show the same trend. The computation of NMR coupling constants is still not frequent for systems of this size and nature,[56] and thus the reliability of the computed DFT $J_{C-H}$ is not well established.[57] The $J_{C-H}$ values are calculated to be 138 and 175 Hz for the *syn* and the *anti* isomers. The measured $J_{C-H}$ for the *syn* isomer of 115 Hz is 23 Hz lower than the calculated value.[58] This illustrates the difficulty in calculating $J_{C-H}$ coupling constants, and it is in particular known that larger basis sets than those used in this work are necessary.[59−61] As often, trends are obtained with higher accuracy than absolute values. $J_{C-H}$ for the *anti* isomer is calculated to be 37 Hz higher than for the *syn* isomer, which is in good agreement with measured $J_{C-H}$ values in the systems where the *syn* and *anti* isomers have been characterized (see below). Test $J_{C-H}$ calculations using single-point DFT calculations on QM/MM-optimized geometries do not improve the results.

The *syn* isomer $\mathbf{1s_q}$ is 2.2 kcal $mol^{-1}$ more stable than the *anti* isomer $\mathbf{1a_q}$. A similar result is obtained from the calculated Gibbs free energies (Table 1). The inclusion of the actual substituents at the QM/MM level slightly stabilizes the *syn* isomer, **1s** being 2.7 kcal $mol^{-1}$ more stable than **1a**. Both results are in agreement with the experimental evidence, since in the case of Re(≡C*t*Bu)(=CH*t*Bu)($CH_2$*t*Bu)$_2$ the *syn* isomer is the only one observed (Table 1). The energy preference for $\mathbf{1s_q}$ over $\mathbf{1a_q}$ can be understood assuming that the α-C−H agostic interaction is stronger than the α-C−C agostic one as the relative elongation of the C−H bond length is larger, the M···H distance is shorter, and the electron density of the C−H bond is more accessible by the metal. The bulky groups in the QM/MM calculations strengthen the α-C−H agostic of the *syn* isomer and suppress the α-C−C agostic interaction, hence increasing the difference in energy between the two rotamers.

To analyze the effect of the ancillary ligands X and Y, we have studied Re(≡C*t*Bu)(=CH*t*Bu)($CH_2$*t*Bu)(OSi$Ph_3$) (**2**) and Re(≡C*t*Bu)(=CH*t*Bu)(O*t*Bu)$_2$ (**3**). Figure 2 shows the optimized geometries, and Table 2 the corresponding relative energies and selected spectroscopic properties. Replacement of alkyl ligands by weak σ-donor/π-donor OR ligands does not substantially modify the coordination geometry at the rhenium center. The alkylidene and alkylidyne ligands remain coplanar, and the angle between them is close to 100° for the QM models ($\mathbf{2s_q}$, $\mathbf{2a_q}$, $\mathbf{3s_q}$, and $\mathbf{3a_q}$). The structural changes concern mainly the α-agostic interaction. The change of an alkyl for a siloxy ligand weakens the C−H and C−C agostic interactions in both the *syn* ($\mathbf{2s_q}$) and the *anti* ($\mathbf{2a_q}$) isomers, as traced by the geometrical parameters related to the agostic interaction. For example, in the comparison of complexes $\mathbf{2_q}$ and $\mathbf{1_q}$, $\mathbf{2s_q}$ presents a larger Re−C2−H angle (107.2° vs 104.2°), a shorter C2−H bond length (1.110 vs 1.112 Å), and a longer Re···H distance (2.444 vs 2.391 Å) than those optimized for $\mathbf{1s_q}$. The agostic interaction becomes even weaker when the two alkyl ligands have been substituted by two alkoxy groups. The inclusion of the full ligands for a better representation of the steric bulk (**2s**, **2a**, **3s**, and **3a**) has an effect similar to that in Re(≡C*t*Bu)(=CH*t*Bu)($CH_2$*t*Bu)$_2$, strengthening the C−H agostic and weakening the C−C agostic interaction in the *syn* and *anti* isomers, respectively, when compared to the QM models.

The computed spectroscopic results for species **1**, **2**, and **3** are similar. The stretching frequencies $\nu_{C-H}$ are smaller for the *syn* isomers than for the *anti* isomers. Similarly the calculated $J_{C-H}$ values are also smaller for the *syn* isomers. While no experimental data are available for the stretching frequencies, experimental $J_{C-H}$ coupling constants are available for the *syn* and the *anti* isomers for comparison with calculated values. The calculated $J_{C-H}$ are too large by around 30−40 Hz, but the difference between the $J_{C-H}$ of the *syn* and *anti* isomers is 40 Hz for species $\mathbf{2_q}$ and 32 Hz for $\mathbf{3_q}$, in very good agreement with the experimental difference of 43 and 37 Hz.[17] More benchmarking calculations on species of this size and nature are needed for assigning the validity of DFT in calculating accurate $J_{C-H}$ coupling constants.[57] Focusing on the *syn* isomers, the experimental values and the calculations show that the $J_{C-H}$ coupling constant slightly increases from **1** to **2** and **3**.

(55) Scott, A. P.; Radom, L. *J. Phys. Chem.* **1996**, *100*, 16502.
(56) Selected list: (a) Khandogin, J.; Ziegler, T. *J. Phys. Chem. A* **2000**, *104*, 113. (b) Bacskay, G. B.; Bytheway, I.; Hush, N. S. *J. Am. Chem. Soc.* **1996**, *118*, 3753. (c) Autschbach, J.; Le Guennic, B. *J. Am. Chem. Soc.* **2003**, *125*, 13585.
(57) Vaara, J.; Jokisaari, J.; Wasylishen, R. E.; Bryce, D. L. *Prog. Nucl. Magn. Res. Spectrosc.* **2002**, *41*, 233.
(58) This $J_{C-H}$ coupling constant has been measured directly in the $^1H$ NMR of the $^{13}C$-labeled compound,[26] which differs from 121 Hz reported by Edwards et al.[14]
(59) Helgaker, T.; Jaszuński, M.; Ruud, K. *Chem. Rev.* **1999**, *99*, 293.
(60) Lutnæs, O. B.; Ruden, T. A.; Helgaker, T. *Magn. Reson. Chem.* **2004**, *42*, S117.
(61) Peralta, J. E.; Scuseria, G. E.; Cheeseman, J. R.; Frisch, M. J. *Chem. Phys. Lett.* **2003**, *375*, 452.

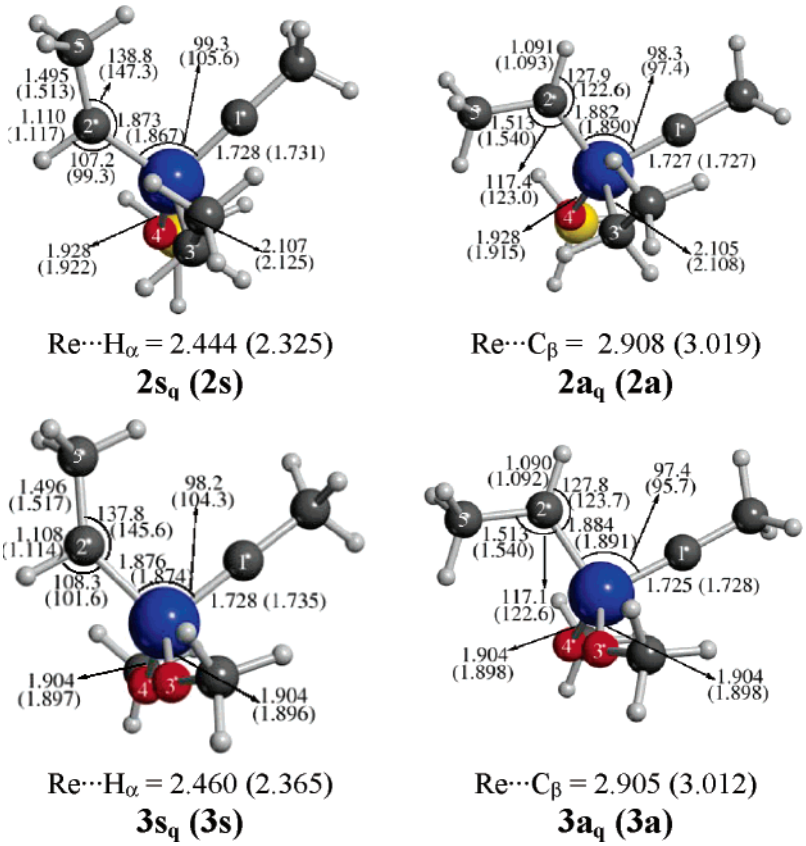


**Figure 2.** Optimized structures of Re(≡CR)(=CHR)($CH_2$R)(OSiR′$_3$) (**2**) and Re(CR)(=CHR)(OR)$_2$ (**3**) using the QM model (R = $CH_3$, R′ = H). The corresponding values from the QM/MM calculations on the full **2** and **3** systems are given in parentheses (*t*Bu and phenyl substituents not shown). Distances in Å and angles in deg.

**Table 2. Energies and Gibbs Free Energies, in kcal mol$^{-1}$, Relative to the More Stable Isomer, Unscaled Stretching Frequencies for C2−H ($\nu_{C-H}$) and C2−C5 ($\nu_{C-C}$) in cm$^{-1}$, and Calculated C2−H NMR Coupling Constants ($J_{C-H}$) in Hz for Re(≡C*t*Bu)(=CH*t*Bu)($CH_2$*t*Bu)(OSiPh$_3$) (2) and Re(≡C*t*Bu)(=CH*t*Bu)(O*t*Bu)$_2$ (3) (experimental $J_{C-H}$ values are added)**

| structure[a] | $\Delta E$ / $\Delta G^\circ_{298}$ | *syn/anti* % calc[b] | *syn/anti* % exptl | $\nu_{C-H}$ calc | $\nu_{C-C}$ calc | $J_{C-H}$ calc | $J_{C-H}$ exptl |
|---|---|---|---|---|---|---|---|
| **2s$_q$** | 0.0 / 0.0 | 88 / 94 | 90 | 2955 | 1154 | 140 | |
| **2a$_q$** | 1.2 / 1.6 | 12 / 6 | 10 | 3154 | 1068 | 180 | |
| **2s** | 0.0 / 0.0 | 78 / 58 | 90 | 2891 | 1087 | | 116 |
| **2a** | 0.7 / 0.2 | 22 / 42 | 10 | 3135 | 1025 | | 159 |
| **3s$_q$** | 0.0 / 0.0 | 67 / 90 | 25 | 2978 | 1157 | 144 | |
| **3a$_q$** | 0.4 / 1.3 | 33 / 10 | 75 | 3161 | 1072 | 176 | |
| **3s** | 1.5 / 1.7 | 8 / 5 | 25 | 2920 | 1086 | | 120 |
| **3a** | 0.0 / 0.0 | 92 / 95 | 75 | 3137 | 1027 | | 157 |

[a] See Figure 2. [b] Calculated from $\Delta E/\Delta G^\circ_{298}$.

The same trend is given for $\nu_{C-H}$. These two trends indicate the decrease of the α-C−H agostic interaction on going from **1** to **3**.

The relative percentage of *syn* and *anti* isomers calculated from $\Delta E$ and $\Delta G^\circ_{298}$ are similar and in good agreement with the experimental data (Table 2). In the small QM model, the preference for the *syn* isomer decreases from **1** to **2** to **3**. Taking into account the full nature of the ligands in the QM/MM calculations, the percentage of *syn* isomers decreases from **1** to **2**, and the *anti* isomer becomes more stable in the case of **3**, in agreement with the experimental data. QM calculations thus show that the decreased preference for the *syn* isomer upon going from **1** to **3** has an electronic origin and the QM/MM calculations show that the steric factors switch the preference between *syn* and *anti* isomers in **3**. It should be pointed out that the differences of energies ($\Delta E$ and $\Delta G^\circ_{298}$) that we have calculated are very small so that the agreement between the experimental and calculated systems is remarkable and should be viewed as fortuitous. However, similar remarkable agreements have been previously found in the experimental and computational studies of Nb complexes with competing α- and β-C−H agostic interactions.[62,63] This shows a remarkable ability of the DFT and QM/MM calculations in estimating accurately differences between isomers with different agostic interactions.

Although the changes of properties ($E$, $\nu_{C-H}$, $J_{C-H}$) between **1**, **2**, and **3** are small, they all indicate the same

(62) Jaffart, J.; Mathieu, R.; Etienne, M.; McGrady, J. E.; Eisenstein, O.; Maseras, F. *Chem. Commun.* **1998**, 2011.
(63) Jaffart, J.; Etienne, M.; Maseras, F.; McGrady, J. E.; Eisenstein, O. *J. Am. Chem. Soc.* **2001**, *123*, 6000.

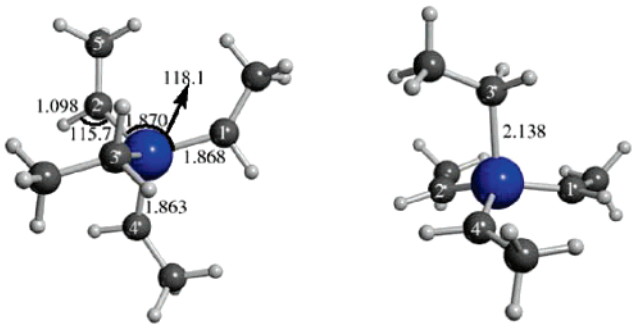


**Figure 3.** Two views of the optimized tris-alkylidene isomer $\mathbf{4_q}$, $Re(CHCH_3)_3(CH_2CH_3)$, and its relative energy to $\mathbf{1s_q}$. Distances in Å and angles in deg.

trend. The *syn* isomer has an α-C−H agostic interaction from the alkylidene group, which does not exist in the *anti* isomer. The strength of the agostic interaction decreases as alkyl groups are replaced by one siloxy and then by two alkoxy groups. It is thought that agostic interactions are favored by an electron-deficient metal. The NPA charge on the rhenium center increases from $\mathbf{1s_q}$ (0.81) to $\mathbf{2s_q}$ (0.94) to $\mathbf{3s_q}$ (1.20), showing that the charge increases with the number of electronegative atoms in the first coordination sphere of the metal. This variation in charge therefore does not rationalize the decrease in the strength of the agostic interaction. In contrast, the $\pi$-donating ability of the ligands correlates with the change in the agostic interaction: the alkyl groups in **1** are pure $\sigma$-donor ligands, and the siloxy group of **2** is a weaker $\pi$-donor ligand than the two alkoxy groups of **3**. Increasing the $d_\pi/p_\pi$ interactions from **1** to **2** and **3** decreases the weak α-C−H agostic interaction and the *syn*/*anti* ratio. We will discuss later how the $\pi$-donating ability of the ligand influences the α-C−H agostic interaction by influencing the shape and energy of the frontier metal d orbitals of the complexes.

**Fluxionality of [Re(≡C*t*Bu)(=CH*t*Bu)($CH_2$*t*Bu)$_2$].** It has been established that the interconversion between *syn* and *anti* isomers is slow and that heating is necessary. Interconversion can occur via the rotation of the alkylidene group or via hydrogen transfer between ligands.[17] Nonetheless, isotope labeling has shown that H scrambling occurs very slowly in all Re(≡CR)(=CHR)(X)(Y) complexes.[19,26] Scheme 2 shows the different fluxionality paths. The rotation of the alkylidene connects directly *syn* and *anti* isomers, and we studied this process for $\mathbf{1_q}$, $\mathbf{2_q}$, and $\mathbf{3_q}$ to analyze the influence of X and Y ligands. Enthalpies for alkylidene rotation have been established for Re(≡C*t*Bu)(=CH*t*Bu)$(OR)_2$ where R = *t*Bu, $CMe_2CF_3$, and $CMe(CF_3)_2$ to be equal to 19.5, 23.4, and 25.5 kcal mol$^{-1}$, indicating an increase of the energy barrier with more electron-withdrawings alkoxy groups.[17] The H transfer process has been computationally analyzed only in $Re(\equiv C-CH_3)(=CHCH_3)(C_2H_5)_2$, where H transfer occurs between all ligands: alkyl/alkylidene, alkylidene/alkylidyne, and alkyl/alkylidyne, the latter forming a tris-alkylidene isomer of the reactant, $Re(=CHR)_3(CH_2R)$, **4** (Figure 3). All studies have been limited to the small systems at the QM level.

Figure 4 gives the geometries of the transition states $\mathbf{TS_{rot}}\boldsymbol{n_q}$ ($n$ = 1, 2, 3) and the rotational barriers of the alkylidene group in $\mathbf{1_q}$, $\mathbf{2_q}$, and $\mathbf{3_q}$. In all cases, the rotation of the alkylidene preserves the tetrahedral coordination at the metal center, but noticeable geometrical changes occur at the alkylidyne and alkylidene groups. At the transition states, the Re−C distances increased for both the alkylidyne and the alkylidene ligands. For instance on going from $\mathbf{1s_q}$ to $\mathbf{TS_{rot}1_q}$, the two Re−C bonds elongate by 0.04 Å. The C1−Re−C2 angle opens and becomes larger than 109°. The alkylidyne bends significantly with an angle Re−C2−C5 of 154.6°. The energy barrier for the alkylidene rotation is high since $\mathbf{TS_{rot}1_q}$ is 22.8 kcal mol$^{-1}$ higher in energy than $\mathbf{1s_q}$, supporting a slow *syn*/*anti* interconversion. Similar geometrical patterns are obtained for $\mathbf{TS_{rot}3_q}$, and the energy barrier is 24.3 kcal mol$^{-1}$. The results are more unusual for $\mathbf{TS_{rot}2_q}$. Because of the presence of two inequivalent substituents, the rotational barriers are different for the two rotational directions. The lower barrier is 29.4 kcal mol$^{-1}$, and the higher one is 36.1 kcal mol$^{-1}$. The lower transition state ($\mathbf{TSrot2_q(1)}$) has an unusual geometry around the alkylidene group with an exceptionaly reduced Re−C−H angle indicative of a very strong agostic interaction. As a consequence, the Re−C(alkylidene) is shortened at the transition state in place of being elongated. In the higher transition state ($\mathbf{TSrot2_q(2)}$), this unusual feature is not present, and the transition state resembles that found for $\mathbf{TS_{rot}1_q}$.

The calculated rotational barrier for $\mathbf{3_q}$ (24.3 kcal mol$^{-1}$) is reasonably close to the enthalpy of rotation measured by NMR for Re(≡C*t*Bu)(=CH*t*Bu)(O*t*Bu)$_2$ (19.5 kcal mol$^{-1}$).[17] In addition, the experimental barrier for the alkylidene rotation increases when the $\sigma$-donor properties of the ancillary ligands decrease (the enthalpy of rotation is 23.4 and 25.5 kcal mol$^{-1}$ for three and six fluorines on the alkoxy ligands, respectively).[17] The same trend is obtained in the calculations as it can be seen by comparing species **1** and **3**. We will discuss later the origin of this hindered rotation (vide infra).

Figure 5 presents the transition states associated with the hydrogen exchange between the ligands in $\mathbf{1_q}$. The transition state $\mathbf{TS5s_q}$ is associated with the transfer of H from an alkyl to the alkylidene group, in which the tetrahedral coordination at Re is retained. The most important geometrical changes are associated with the carbon atoms involved in the hydrogen exchange. The Re−C2 distance increases while the Re−C4 distance decreases, yielding a transition state structure with almost equal Re−C2 and Re−C4 distances, with values intermediate between Re−C double and single bonds. The C2−Re−C4 angle is more open in the transition state (108.5° for reactants, 113.9° for $\mathbf{TS5s_q}$, and 107.3° for products), leading to long distances between the migrating H and the two carbons (1.845 Å from C4 and 1.833 Å from C2). The energy of $\mathbf{TS5s_q}$ is 40.5 kcal mol$^{-1}$ above $\mathbf{1s_q}$, indicating a high-energy process.

The transfer of a hydrogen between one alkyl and the alkylidyne group gives a tris-alkylidene product, $Re(=CHCH_3)_3(CH_2CH_3)$, $\mathbf{4_q}$, whose structure corresponds to a tetrahedron flattened toward a trigonal prism geometry, in which the alkyl group is the apical ligand and the three alkylidene groups are at the basal

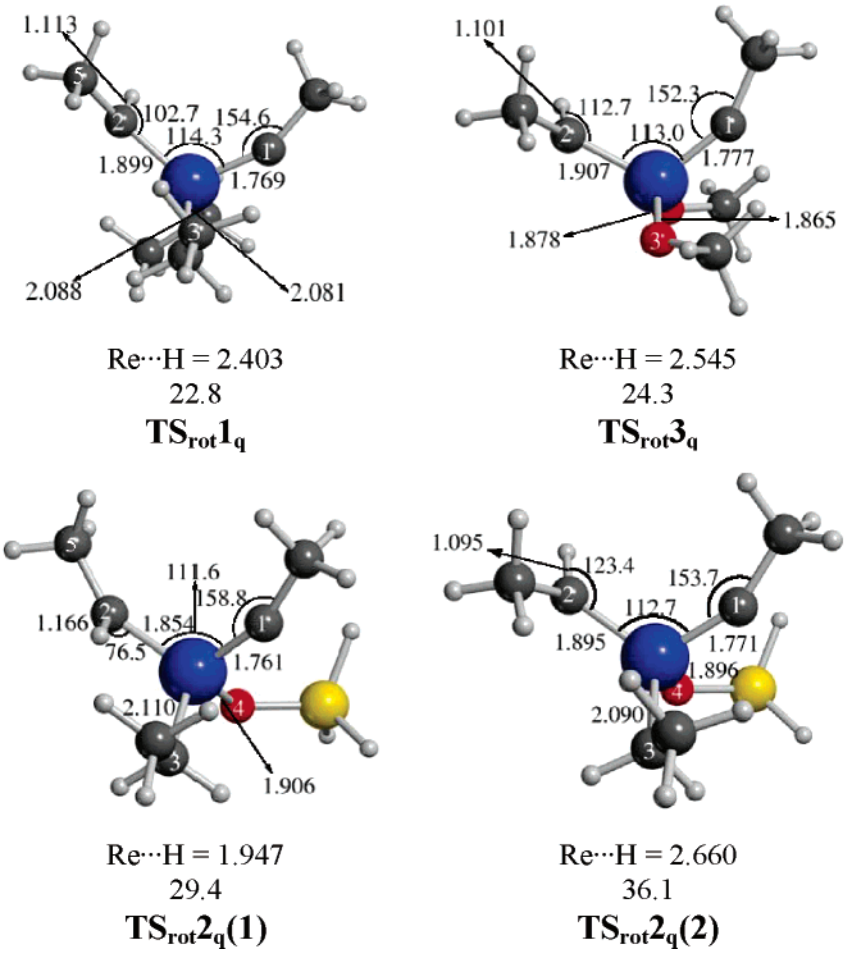


**Figure 4.** Transition state structures for the alkylidene rotation in $\mathbf{1}_q$, $\mathbf{2}_q$, and $\mathbf{3}_q$ and their energies (kcal mol$^{-1}$) relative to the *syn* isomers. Distances in Å and angles in deg.

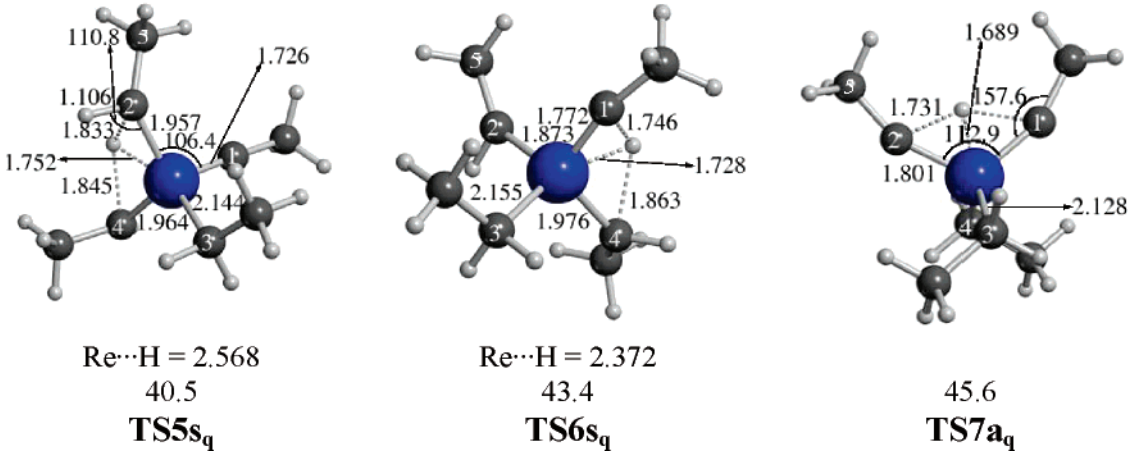


**Figure 5.** Transition state structures for H transfer between alkyl, alkylidene, and alkylidyne ligands and their energies (kcal mol$^{-1}$) relative to $\mathbf{1s}_q$. Distances in Å and angles in deg.

sites (C4−Re−C$_{ene}$ average angle is equal to 103.6°). The $\pi$ orbitals of alkylidene ligands are almost parallel to the Re−C4 direction. The energy of $\mathbf{4}_q$ is 5.5 kcal mol$^{-1}$ above $\mathbf{1s}_q$. Similar energy preferences for alkylidyne-alkyl over bisalkylidene complexes have been found.[64] The transition state $\mathbf{TS6s}_q$, which connects $\mathbf{1s}_q$ to $\mathbf{4}_q$, has a geometry intermediate between $\mathbf{1s}_q$ and $\mathbf{4}_q$. The Re−C1 bond is intermediate between Re−C triple and double bonds, and the Re−C3 is intermediate between Re−C double and single bonds. The exchanging hydrogen is quite far from both the two carbons (1.746 and 1.863 Å). The energy barrier is 43.4 kcal mol$^{-1}$, also indicating a high-energy process.

The transition state $\mathbf{TS7a}_q$ for the transfer of H between the alkylidene and the alkylidyne has essentially a mirror plane: the Re−C2 and Re−C1 distances are intermediate between Re−C double and

(64) Choi, S.-H.; Lin, Z.; Xue, Z. *Organometallics* **1999**, *18*, 5488.

triple bonds. The transferring H is far from C2 and C1 so that **TS7a$_q$** is also high in energy (45.6 kcal mol$^{-1}$).

It appears that the transfer of hydrogen between any ligand is associated with high-energy barriers, indicating very slow isotope scrambling, in good agreement with experimental data.[19,26] The rotation around the alkylidene group has a much lower barrier and is the preferred fluxional process, and accounts for the *syn*/*anti* interconversion upon heating. The high-energy barriers associated with the H transfer between the perhydrocarbyl ligands as calculated in **1$_q$** are in agreement with the rarity and slowness of α-H transfer processes.[36,64−67]

**Interpretation of the Structure and Fluxionality of Re(≡C*t*Bu)(=CH*t*Bu)(X)(Y) Complexes.** The alkylidyne-alkylidene rhenium complex is formally a 14-electron complex and is therefore unsaturated. However, formal electron counting has no relation with the charge at the metal center, which may represent better the properties of the complex. The NPA charge on rhenium increases from 0.8 to 0.9 and to 1.2 for the series **1s$_q$**, **2s$_q$**, and **3s$_q$**, indicating that the metal is more electron poor in the presence of the alkoxy ligands than in the presence of the alkyl ligands, the species with the siloxy group being intermediate. This shows that the total charge at the metal is driven by the electron-accepting ability of the alkoxy group and not by the d$_\pi$/p$_\pi$ donation from the oxygen lone pair. However, this criterion cannot explain two results: the presence of an α-C−H agostic interaction in the *syn* isomer only and the decrease of the strength of the agostic interaction with an increasing number of OR groups. The lack of relation between the agostic interaction and the charge on the metal shows that the agostic interaction does not have an electrostatic origin. It has been recognized that an agostic interaction requires an empty coordination site with strong acidic Lewis character (i.e., a low lying empty orbital that interacts with the C−H bond acting as a Lewis base),[38] yet a nondistorted tetrahedral complex does not have in principle an empty coordination site.[30] We will thus use a molecular orbital diagram to show that a given structural deformation is favorable to the occurrence of a low lying empty orbital that interacts with the (=C−H) bond in the *syn* geometry only.

An ideal $T_d$ ligand field, set by the four $\sigma$ bonds between Re and the four ligands, is used as a reference (Figure 6). From this ideal situation, a Walsh diagram is constructed to follow the energy of the five 5d orbitals as a function of the angle C1−Re−C2 between the alkylidyne and alkylidene ligands. In Figure 7, the $\pi$ interactions between the metal, the alkylidene, and the alkylidyne orbitals are considered in two conformations: the coplanar experimentally preferred conformation (left-hand side) and the perpendicular conformation (right-hand side) corresponding to the transition state for the *syn*/*anti* interconversion. Following the conventions, the alkylidene is a CHR$^{2-}$ ligand and the alkylidyne a CR$^{3-}$ ligand; hence the $\pi$ orbitals of the two ligands are doubly occupied.

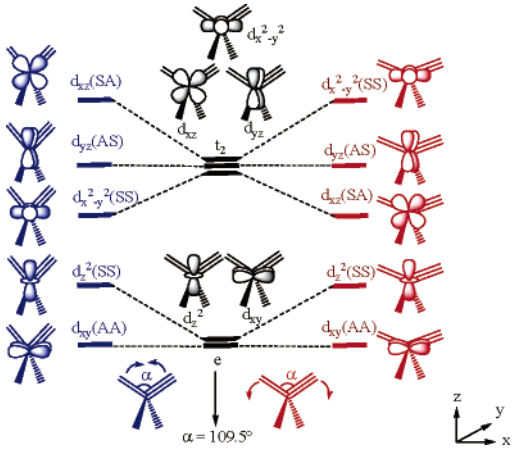


**Figure 6.** Walsh diagram for the metal d orbitals of a tetrahedral complex as a function of the angle between the alkylidene and alkylidyne ligands. The energy scale is qualitative.

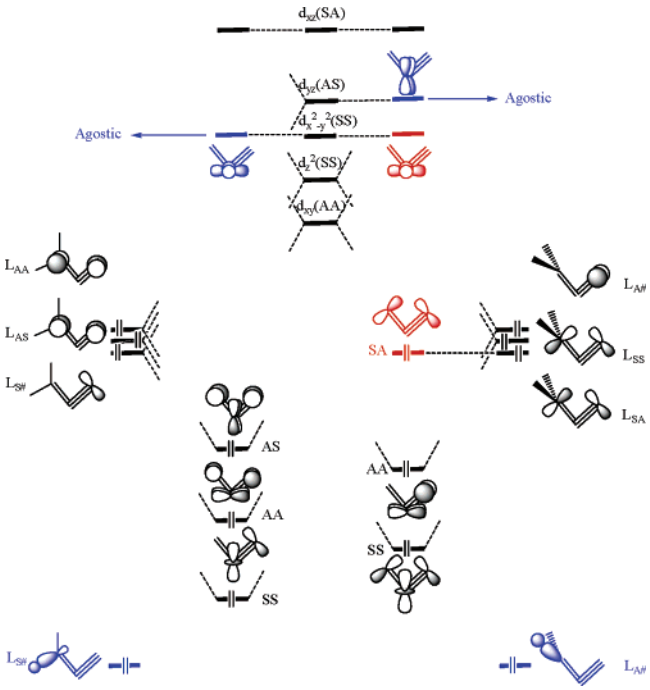


**Figure 7.** Interaction diagram showing the Re−C multiple bonds and the agostic interaction in the coplanar (left) and perpendicular (right) orientation. The energy scale is qualitative.

When the C1−Re−C2 angle departs from 109°, the degeneracy within the e$_g$ and t$_2$ orbitals is raised. The 5d$_{xy}$ and 5d$_{yz}$ orbitals are not affected by a change in the C2−Re−C1 angle. The decrease of the C1−Re−C2 angle stabilizes 5d$_{x^2-y^2}$ because the out-of-phase interaction between Re and the two ligands decreases. For the same angular variation, 5d$_{z^2}$ and specifically 5d$_{xz}$ are destabilized. Conversely, when the C1−Re−C2 angle increases, 5d$_{xz}$ is stabilized, while 5d$_{z^2}$ and 5d$_{x^2-y^2}$ are destabilized.

The d$_\pi$/p$_\pi$ interaction is added to the metal d orbitals in the coplanar orientation, and the qualitative features do not depend on the C1−Re−C2 angle. The alkylidene and alkylidyne $\pi$ orbitals mix to be adapted to the

(65) (a) Chen, T.; Wu, Z.; Li, L.; Sorasaenee, K. R.; Diminnie, J. B.; Pan, H.; Guzei, I. A.; Rheingold, A. L.; Xue, Z. *J. Am. Chem. Soc.* **1998**, *120*, 13519. (b) Morton, L. A.; Zhang, X.-H.; Wang, R.; Lin, Z.; Wu, Y.-D.; Xue, Z.-L. *J. Am. Chem. Soc.* **2004**, *126*, 10208.

(66) Fellmann, J. D.; Schrock, R. R.; Traficante, D. D. *Organometallics* **1982**, *1*, 481.

(67) Morris L. J.; Downs, A. J.; Greene, T. M.; McGrady, G. S.; Herrmann, W. A.; Sirsch, P.; Gropen, O.; Scherer, W. *Chem. Commun.* **2000**, 67.

approximate symmetry of the complex with respect to the *xz* and *xy* planes. Thus the in-phase and out-of-phase combinations of the $p_y$ orbitals of the two ligands are $L^C_{AS}$ and $L^C_{AA}$, where the labels indicate the symmetry with respect to the *xz*/*yz* planes and C stands for coplanar. The other $\pi$ orbital of the alkylidyne, in the *xz* plane, does not combine in any significant manner with an orbital on the alkylidene ligand and is thus labeled as $L^C_{S\#}$. The metal d orbitals combine with the three ligand $\pi$ orbitals to form three Re−C $\pi$ bonds: $5d_{xy}$ and $5d_{yz}$ combine with $L^C_{AA}$ and $L^C_{AS}$, respectively, and $5d_{z^2}$ has the nodal properties to fit $L^C_{S\#}$. This leaves two metal d orbitals for additional interactions ($5d_{x^2-y^2}$ and $5d_{xz}$). In the case of a small C1−Re−C2 angle, $5d_{x^2-y^2}$ is at relatively low energy and is spatially well adapted to interact with the C−H bond, which lies in the *xz* plane, giving rise to the C−H agostic interaction for the *syn* isomer. In the case of a large C1−Re−C2 angle, the $5d_{x^2-y^2}$ is at higher energy and the $5d_{xz}$ is not so well directed to overlap with the C−H bond, so that no C−H agostic interaction can be implemented.

In summary three Re−C $\pi$ bonds can be implemented for the *syn* and *anti* orientations. In addition, for the *syn* isomer, a decrease of the C1−Re−C2 angle lowers a metal d orbital that is spatially well adapted to be reached by the C−H bond, giving rise to an α-C−H agostic interaction. In the *anti* isomer, the C−C bond can make an agostic interaction, while the C−H bond no longer finds an accessible empty metal d orbital. This molecular orbital analysis shows that the Re−C multiple bonds of the alkylidyne and alkylidene can be combined with an α-C−H agostic bond in quasi-tetrahedral complexes for a specific orientation of the ligands. This clearly indicates a different electronic situation from that of regular tetrahedral complexes such as $Cl_3TiMe$, for which no agostic interaction is observed. In the complex with the full substituent set, the steric factors open the C1−Re−C2 angle to diminish the repulsion between the bulky groups on the alkylidyne and alkylidene. This disfavors the C−H agostic interaction, but this is compensated by an increase in the C5−C2−Re angle, which brings the C−H bond of the alkylidene closer to the metal center.

Figure 8 shows the actual orbitals responsible for the three occupied Re−C $\pi$ bonds. The close proximity in energy of the two lower orbitals (labeled SS and AA) comes from the relatively close proximity in energy of the $5d_{xy}$ and $5d_{z^2}$ orbitals (Figures 6 and 7). The AS orbital is significantly higher because of the higher energy of $5d_{yz}$, which stabilizes less efficiently the ligand $\pi$ orbitals. The C−H agostic interaction could be identified only through the out-of-phase combination of the metal orbital (a distorted $5d_{x^2-y^2}$) and the C−H contribution because the in-phase combination is diluted among many occupied orbitals.

Rotating the alkylidene group modifies first the Re−C $\pi$ bonding. The in-phase and out-of-phase combinations of the alkylidene and alkylidyne $\pi$ orbitals lie in the *xz* plane and are labeled $L^P_{SS}$ and $L^P_{SA}$ (where P stands for perpendicular). The isolated $\pi$ orbital of the alkylidyne is perpendicular to the *xz* plane and is labeled $L^P_{A\#}$. The $L^P_{SA}$ orbital does not find a good match with the metal orbital and thus remains nonbonding with respect to the metal. The two other ligand orbitals $L^P_{SS}$ and $L^P_{A\#}$

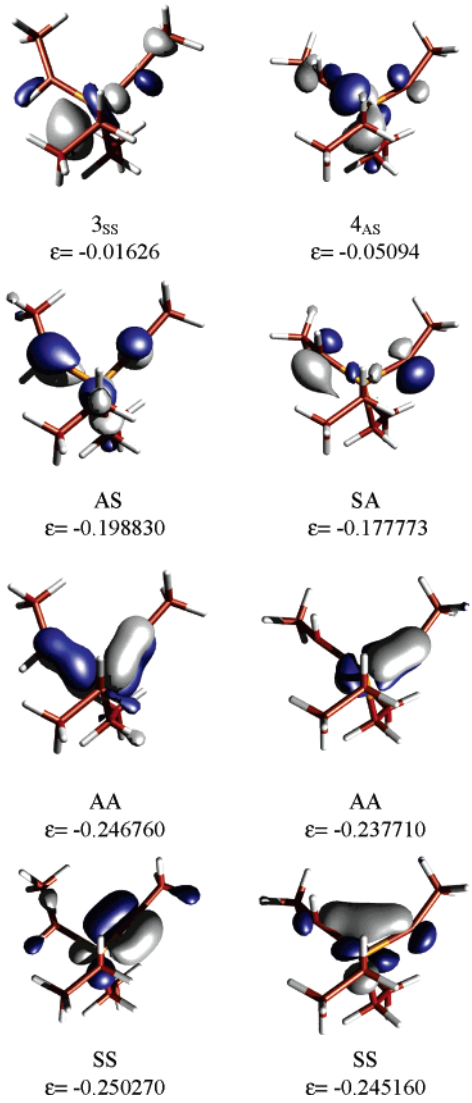


**Figure 8.** Molecular orbitals for the *syn* isomer (left) and transition state structure for alkylidene rotation (right) of $Re(\equiv CCH_3)(=CHCH_3)(CH_2CH_3)_2$.

match $5d_{xy}$ and $5d_{z^2}$, and four electrons are thus stabilized, giving rise formally to two Re−C $\pi$ bonds in place of three $\pi$ bonds in the coplanar geometry. Thus going from the ground state $\mathbf{1s_q}$ to the transition state $\mathbf{TS_{rot}1_q}$ results in the loss of Re−C $\pi$ bonding. The energy barrier for the alkylidene rotation is in fact quantitatively determined by the energy of the Re−C $\pi$ bonds. The sum of the three occupied orbitals describing the $\pi$ orbitals of the alkylidene and the alkylidyne ligands in the coplanar arrangement is 22.1 kcal $mol^{-1}$ more stable than the sum of the two Re−C $\pi$ orbitals and the nonbonding orbital located on the alkylidyne and the alkylidene. While such quantitative agreement is somewhat fortuitous, it clearly shows that these three orbitals have a determinant role in the alkylidene rotation barrier. Similar qualitative arguments have been proposed in related isoelectronic imido-alkylidene Mo and W complexes.[33]

The Re-alkylidyne and the Re-alkylidene bonds are both elongated by the alkylidene rotation because the $L^P_{SA}$ orbital is delocalized on the two ligands. The $L^P_{SA}$ orbital is out-of-phase between the carbons of the alkylidene ($C_{ene}$) and alkylidyne ($C_{yne}$) ligands, which

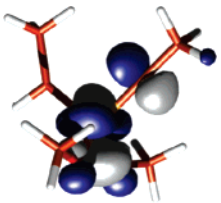

$3_{ss}$

**Figure 9.** Lowest vacant molecular orbital in $\mathbf{3s_q}$ with the appropriate symmetry to interact with the C−H bond and showing preferred mixing with the oxygen lone pair (out-of-phase combination shown).

induces an opening of the C1−Re−C2 angle to decrease the antibonding interaction. Furthermore, this orbital is also stabilized by mixing in some $\sigma$ character, especially at the carbon of the alkylidyne group, where sp mixing is stronger. This causes the bending of the alkylidyne ligand. The C−H agostic interaction is not excluded in the perpendicular orientation $\mathbf{TS_{rot}1_q}$ because the C−H bond can interact with the metal d orbital left unused by the $d_\pi/p_\pi$ interactions.

The DFT calculations have indicated that the strength of the agostic interaction decreases when the ancillary alkyl ligands are replaced by OR groups. We have seen how the agostic interaction could result from the interaction in the *syn* isomer of the C−H bond with a relatively low lying $5d_{x^2-y^2}$ orbital. The C−H bond is a poor electron donor, and therefore the oxygen lone pair, a better electron donor, replaces the α agostic interaction. This is illustrated by the shape of the molecular orbital $d_{x^2-y^2}$ in $\mathbf{3s_q}$, in which the C−H contribution has been replaced by the oxygen lone pair (Figure 9). A similar behavior has been noted in Tp′Ta(=CH-*t*Bu)(X)(Y) (Tp′ = hydrotris(3,5-dimethylpyrazolyl)borate), X = Y = halide, OR, $NR_2$), where the C−H agostic interaction decreases with increasing $\pi$ donation.[68]

The effect of the X and the Y groups on the rotational barrier of the alkylidene group is more difficult to establish because of the unusual barrier found for $\mathbf{2_q}$ (X = alkyl, Y = $OSiH_3$). Therefore, we focus on the comparison between $\mathbf{1_q}$ (X = Y = $CH_2CH_3$) and $\mathbf{3_q}$ (X = Y = $OCH_3$). The higher barrier for $\mathbf{3_q}$ agrees with the experimental observation of increasing rotational barrier upon increasing fluorination of the alkoxy group.[17] An alkyl group is a pure $\sigma$-donor group, while an alkoxy group is both a weak $\sigma$-donor and a $\pi$-donor group. If the weak $\sigma$-donor character of the ligand dominates, this reinforces, by synergy, all metal−ligand $\pi$ bonds and in particular the Re−C $\pi$ bonds because C-based ligands are better electron donors than O-based ligands. If the $\pi$-donating effect dominates, this weakens the Re−C $\pi$ bonds. In the first case, the rotational barrier should increase, while it should decrease in the second case. In Table 3 are reported the NPA charges for $\mathbf{1s_q}$ and $\mathbf{3s_q}$. The substitution of X = $CH_2CH_3$ by the more electron-withdrawing $OCH_3$ groups leads to an increase of the positive charge at Re, i.e., + 0.4e⁻, and also to an increase of negative charge at the *four* atoms directly bonded to Re, i.e., −0.1e⁻. Thus the replacement of $CH_2$-$CH_3$ by $OCH_3$ increases the ionic character of all metal−ligand bonds. No change in electron density is found on atoms not bonded to the metal.

**Table 3. NPA Charges for $\mathbf{1s_q}$, $\mathbf{TS_{Rot}1s_q}$, $\mathbf{3s_q}$, and $\mathbf{TS_{Rot}3s_q}$**

| | $\mathbf{1s_q}$ | $\mathbf{TS_{rot}1_q}$ | $\mathbf{3s_q}$ | $\mathbf{TS_{rot}3_q}$ |
|---|---|---|---|---|
| Re | 0.808 | 0.817 | 1.196 | 1.292 |
| $C_{ene}$ | −0.412 | −0.591 | −0.474 | −0.608 |
| $H_{ene}$[a] | 0.212 | 0.238 | 0.216 | 0.247 |
| $CH_{3,ene}$[a] | 0.007 | 0.002 | −0.003 | 0.004 |
| $C_{yne}$ | 0.002 | −0.113 | −0.106 | −0.265 |
| $CH_{3,yne}$[a] | 0.007 | −0.018 | 0.008 | −0.017 |
| X | −0.311 | −0.154 | −0.420 | −0.336 |

[a] $H_{ene}$, $CH_{3,ene}$, and $CH_{3,yne}$ stand for the alkylidene α-hydrogen and the methyl groups of the alkylidene and alkylidyne ligands, respectively.

**Table 4. AIM[a] and NBO Analysis for the Re−Alkylidene Bond in $\mathbf{1s_q}$, $\mathbf{TS_{Rot}1s_q}$, $\mathbf{3s_q}$, and $\mathbf{TS_{Rot}3s_q}$**

| | $\mathbf{1s_q}$ | $\mathbf{TS_{rot}1_q}$ | $\mathbf{3s_q}$ | $\mathbf{TS_{rot}3_q}$ |
|---|---|---|---|---|
| $\epsilon^b$ | 0.373 | 0.352 | 0.440 | 0.433 |
| $\rho_c{}^b$ | 0.205 | 0.190 | 0.198 | 0.189 |
| $\nabla^2\rho_c{}^b$ | 0.086 | 0.084 | 0.104 | 0.078 |
| $H_c{}^b$ | −0.139 | −0.123 | −0.132 | −0.121 |
| $\%C_\sigma{}^c$ | 58.6 | 62.9 | 60.3 | 62.7 |
| $\%C_\pi{}^c$ | 56.6 | 64.1 | 54.3 | 62.3 |

[a] All the AIM values are given in atomic units. [b] $\epsilon$, $\rho_c$, $\nabla^2\rho_c$, and $H_c$ are the ellipticity, the density, the Laplacian of the electron density, and the energy at the bond critical point. [c] In the NBO analysis, $\%C_\sigma$ and $\%C_\pi$ are the weight on the alkylidene carbon atom in the $\sigma$ and $\pi$ Re−C bonds as determined by the NBO procedure.

The molecular orbital analysis has shown that rotating the alkylidene group decreases the number of Re−C $\pi$ bonds and forms a high lying molecular orbital essentially located on $C_{ene}$ and $C_{yne}$, where $C_{ene}$ ($C_{yne}$) is the alkylidene (alkylidyne) carbon atom bonded to Re. This is demonstrated in the NBO analysis by an increased negative charge on both $C_{ene}$ (0.2 e⁻) and $C_{yne}$ (0.1e⁻) centers. This is related to what has been suggested in the related imido Mo and W complexes, where the rotation of the alkylidene group induces a relocalization of the electron density on the sole imido N center due to the difference of electronegativity between C and N.[4]

The charge on the metal does not vary much between $\mathbf{1s_q}$ and $\mathbf{TS_{rot}1_q}$ resulting from a larger donation of electron density from X in the transition state. When X is an alkoxy group, the electron donation from X is smaller and the electron density on $C_{ene}$ is larger. This increased charge separation from ground state to transition state in $\mathbf{3s_q}$ compared to $\mathbf{1s_q}$ is associated with a slightly higher barrier for alkylidene rotation.

Table 4 gives the results of atoms-in-molecules (AIM) and natural bonding orbital (NBO) analyses for the Re−alkylidene bond in $\mathbf{1s_q}$ and $\mathbf{3s_q}$ as well as for $\mathbf{TS_{rot}1_q}$ and $\mathbf{TS_{rot}3_q}$. AIM ellipticity $\epsilon$ values clearly indicate that the Re−$C_{ene}$ bond has a marked $\pi$ component in all these systems. They also show that the $\pi$ character of the Re−$C_{ene}$ bond is more pronounced in $\mathbf{3s_q}$ ($\epsilon$ = 0.440) than in $\mathbf{1s_q}$ ($\epsilon$ = 0.373). The negative value of $H_c$ is consistent with a covalent character for the Re−$C_{ene}$ bond, as expected for a Schrock type carbene.[69,70] The values of $\rho_c$ for the Re−$C_{ene}$ bonds are similar to those

(68) Boncella, J. M.; Cajigal, M. L.; Abboud, K. A. *Organometallics* **1996**, *15*, 1905.

(69) Cremer, D.; Kraka, E. *Angew. Chem., Int. Ed.* **1984**, *23*, 627.
(70) Vyboishchikov, S. F.; Frenking, G. *Chem. Eur. J.* **1998**, *4*, 1428.

of simple carbon−carbon bonds in organic systems. In fact, $\rho_c$ values for the $C_{ene}-CH_{3,ene}$, $C_{yne}-CH_{3,yne}$, and $C_{ene}-H_{ene}$ in these complexes are ca. 0.25 au, consistent with their single covalent bond character, as further confirmed by their $\nabla^2\rho_c$ (−0.66 au) and $H_c$ (−0.23 au) values. However, in the case of the $Re-C_{ene}$ bonds, the values for $\nabla^2\rho_c$ and $H_c$ are not characteristic of a single covalent bond. Therefore in terms of the topological properties of the electron density, the $Re-C_{ene}$ bond is best described as a Re=C bond with a partial covalent character. The rotation of the alkylidene ligand does not introduce major changes in the topological properties of the electron density in the $Re-C_{ene}$ bond and, therefore, does not change in a significant manner the nature of this bond. The NBO results also agree with the description of the $Re-C_{ene}$ as a double bond, as two natural bonding orbitals are found between Re and $C_{ene}$. Both orbitals are polarized toward the carbon, as expected for a Schrock type carbene, in agreement with the negative NPA charge on $C_{ene}$ (Table 3). The $\sigma$ bond is built on an $sp^{2.0}$ hybrid on $C_{ene}$, and the $\pi$ bond uses the p AO on $C_{ene}$ perpendicular to the alkylidene plane.

The substitution of $X = CH_2CH_3$ by $OCH_3$ induces a different response of the two NBOs. The $\sigma$ bond is more polarized toward the carbon in **3s$_q$** ($\%C_\sigma = 58.6$, **1s$_q$** vs $\%C_\sigma = 60.3$, **3s$_q$**), in agreement with the increased total NPA charge. In contrast, the $\pi$ bond becomes more delocalized on the carbon and metal as the weight of the $\pi$ character on $C_{ene}$ diminishes in **3s$_q$** ($\%C_\pi = 56.6$, **1s$_q$** vs $\%C_\pi = 54.3$, **3s$_q$**). This indicates that the $\pi$ bond character of the Re−alkylidene bond is increased upon substitution of $X = CH_2CH_3$ by $OCH_3$, as already indicated by the increase ellipticity of the Re=C bond. These results suggest a Re−alkylidene $\pi$ bond more delocalized between Re and C in **3s$_q$** than in **1s$_q$**, which is consistent with the higher barrier of rotation in **3s$_q$**. In conclusion, the inclusion of weak $\sigma$ donor ligands (OR) leads to more ionic Re−L $\sigma$ bonds (both Re−O and Re−C), which is compensated by a reinforcement of Re−C multiple bonds, especially the $Re-C_{ene}$ double bond.

## Conclusions

The DFT and QM/MM calculations of Re(≡CR)(=CHR)(X)(Y) are fully consistent with experimental data. All these complexes adopt a pseudo-tetrahedral structure. An angular distortion at the metal center allows the formation of three metal−carbon $\pi$ bonds and an α agostic interaction with the bond *anti* to the alkylidyne ligand, i.e., the C−H and the C−C bond in the *syn* and *anti* isomers, respectively. The presence of the C−H agostic interactions in the *syn* isomers is evidenced by geometrical features as well as the $\nu$(C−H) and $J_{C-H}$ coupling constants calculated to be lower than in the *anti* isomers, as observed experimentally in the case of the $J_{C-H}$.

The C−H agostic interaction is more stabilizing than the C−C agostic interaction, hence a greater stability of the *syn* isomer. Ancillary X and Y ligands that are weak $\sigma$-donors and $\pi$-donors (OR) compete with the C−H agostic interaction because the oxygen lone pair is a better electron donor to the metal than a C−H bond. Therefore, the *syn* isomer is preferred with ancillary ligands that are pure $\sigma$-donors, while the *anti* isomer becomes increasingly preferred with $\pi$-donor ligands, and the calculated *syn*/*anti* ratio is in good agreement with experimental data.

The *syn*/*anti* inconversion occurs preferentially via the alkylidene rotation, whose energy barrier is high, in agreement with the slow experimental isomerization because of the loss of the $Re-C_{yne}$ and $Re-C_{ene}$ $\pi$ bonds in the transition state. Moreover, H transfers between perhydrocarbyl ligands have much higher energy barriers, showing that these processes do not compete with alkylidene rotation and that α-H scrambling is very slow.

The MO and the electron density analyses show that the strength of the agostic interaction does not increase when the metal becomes more electron poor (ancillary ligands going from alkyl to alkoxy), as indicated by the total charge on the metal center. The agostic interaction is due only to the perturbation of the ligand field away from the tetrahedral geometry.

We are currently studying the structure of the isoelectronic group 6 metal complexes and probing the reactivity of *syn* and *anti* isomers of group 6 and 7 systems in olefin metathesis.[31]

**Acknowledgment.** X.S.M. thanks the CNRS for a postdoctoral position, the IDRIS (grant 041744) and CINES (grant lsd2217) French national computing centers for a generous donation of computer time, and Dr. Ricard Gelabert for helpful discussion.

OM048997S